Laboratory investigation of suction distribution in a modified capillary barrier system

G H Yunusa[1], A Kassim[2], M Umar[1], Z A Talib[3] and A Y Abdulfatah[1]

[1]Department of Civil Engineering, Bayero University Kano, Nigeria, PMB3011, Kano, Nigeria
[2]Department of Geotechnics and transportation, Universiti Teknologi Malaysia, Malaysia
[3]Department of Infrastructure & Geomatic Engineering, Universiti Tun Hussein Onn Malaysia, Malaysia

ghyunusa.civ@buk.edu.ng

Abstract. This paper investigated the effect of transport layer in the diversion capacity of natural capillary barrier system using laboratory slope model. The slope model was constructed with stainless steel and 5 mm thick acrylic sheets. Grade VI and grade V soils classified as sandy silt of very high plasticity (MVS) and silty gravel of high plasticity (MHG), respectively were arranged in the slope model with sand and gravel transport layers sandwiched at their interface. The model was subjected to different rainfall intensities using rainfall simulator to determine the behaviour of water flow and suction distribution in the slope model. The results obtained show a modification in the suction distribution behaviour and the natural capillary barrier effect was sustained. It was also observed that a transport layer formed with gravel material was more effective in diverting the infiltrating water compared to that of gravelly sand. This occurred because the upper grade VI layer possessed capillary forces due to its finer pore structures and relatively large air entry value, thus, it retained the infiltrating water, and the gravel transport layer possessed relatively larger pore structures compared to the grade VI layer and hence it possessed higher hydraulic conductivity values and small water entry value. This arrangement provide a capillary break and allowed the infiltrating water to flow above the interface. Therefore, the inclusion of transport layer provides a definite path through which the infiltrating water flows and diverted laterally. Thus, improving the performance of natural capillary barrier effect.

1. Introduction

In many tropical regions where the residual soil slope frequently exists in unsaturated condition with deep groundwater table, slope failures often occur due to rainfall infiltration [1]. Rainfall infiltration affects both hydraulic and shear strength properties of unsaturated soils, which invariably affect the stability of the soil slope. It eliminates the shear strength of the soil, especially during monsoon seasons when the soil is subjected to prolonged or intense rainfall events [2].

Residual soil is normally considered as the uppermost layer (Grade VI) of the soil profile and consists of materials that are predominantly decomposed to Grade IV and Grade V of the weathering profile. One of the common inherent features of tropical residual soil mantle is heterogeneity, which occurs due to weathering process.

The typical arrangement of Grade VI over Grade V soil layers according to weathering profile, results in fine-grained soil material close to the ground surface compared to soil at greater depth. Thus, fine material content decreases with increase in depth [3]. Most of the rainfall-induced slope failures occur as shallow slope failure within the Grade VI residual soil layer. This is due to the contrast in the hydraulic conductivity between the upper Grade VI residual soil and the lower Grade V layer that impedes downward movement of water and creates an unstable area with locally elevated pore-water pressure. Rahardjo *et al*. [4] analyses 20 rainfall-induced slope failures that occurred in Nanyang Technological University, Singapore and found that 15 out of the 20 occurred within the grade VI residual soil layer, while the remaining occurred at the interface between Grade VI and Grade V. Therefore, the depth to the interface from ground surface has a great influence on stability of slope as it determines the depth of failure of the slope. The top-grade VI residual soil usually slides along the interface of the two layers when the interface lies near the slope surface [4].

The typical arrangement of Grade V and Grade VI soil layers and the inherent feature of heterogeneity in Grade V layer results in contrast in hydraulic conductivity between the soil layers. This in turn forms a system of soil with natural capillary barrier effect, which relies on variation of hydraulic conductivity as function of matric suction potential and creates a capillary break at the interface of grade V and grade VI soil. The capillary break restricts downward movement of water and facilitates lateral flow of water above the interface of the soil layers [5, 6]. A capillary barrier system is an earthen cover which comprises of fine-grained soil layer overlying a coarse-grained soil layer [7-9] and can occur naturally in layered heterogeneous systems or can be an engineered using selected soil material [10–13]. In a capillary barrier system, saturation may occur due to poor drainage along the interface. Once breakthrough occurs, the system becomes ineffective as rainwater will continue to penetrate into deeper depth and eliminates the soil matric suction and cause slope failure.

One of the measures of improving the performance of capillary barrier system is the use of transport layer (also known as unsaturated drainage layer) [5,14]. A transport layer is an intermediate layer of different soil material of relatively high permeability compared to other soil layers and constructed at the finer/coarser interface so that the infiltrating water can flow above and within this layer due to the sloping surface. The difference in particle sizes between the fine-grained soil layer and the transport layer maximizes lateral water diversion in the system [7,15,16]. A system with capillary barrier effects was found to be more effective with transport layer by preventing the development of positive pore-water pressure in response to rainfall infiltration [17]. The material to be used as transport layer should have sufficient moisture to be conductive enough to laterally divert downward moving water and yet remain unsaturated to preserve capillary break within the underlying coarser material [5].

Presently, no much attention was given to the natural capillary barrier phenomena that exist in tropical residual soil mantle, which is quite abundance in tropical regions. Poor drainage in residual soil, renders the capillary barrier phenomena ineffective due to development of positive pore-water pressure in response to rainfall infiltration. The development of positive pore-water pressure results in slope failure that is shallow in nature. Therefore, the poor drainage characteristics of the residual soil mantle can be improved significantly by introducing a transport layer.

2. Laboratory Model Setup

2.1. Material and devices used in the laboratory model construction

The laboratory slope model was 2000 mm in length, 1100 mm in height and 100 mm in width. The model is deemed a two-dimensional model because of the low width to height and length ratios. Therefore, flow of water along the width direction of the model (*y*-axis) was not considered in the study. The frame of the model was made with the stainless steel and it helps in eliminating the possibility of deflection while conducting the experiment. The sidewalls of the model were made with 5 mm thick acrylic sheet, which allows visual observation of wetting front progression during the experiment. Four types of boundary conditions were applied to the slope model. Two of these

boundary conditions were applied during the fabrication process while the remaining boundary conditions are applied while conducting the experiments. The left and right vertical sidewalls of the slope model were designed and constructed as impervious (i.e., a zero-flux boundary, $Q = 0$) and a unit hydraulic gradient flow conditions was assigned at the bottom of the slope model. The third boundary condition; a constant infiltration rate, q was applied on the exposed sloping surface through a rainfall simulator while conducting the experiment. Water that does not gain entry into the soil systems during the test was later discharge as runoff and drained out through the second outlet located at one side of the model, this create no-ponding upper flux boundary condition during the experiment. A total number of 32 threaded holes were drilled at various spacing along the sidewall of the model.

The water flow system consisting of inflow/rainfall control, overflow/runoff discharge, and percolation discharge) was used in the study. The inflow/rainfall control water flow system consisted of two water storage tanks, a constant head tank, a flow regulator (ball cock valve) and a rainfall simulator. The rainfall simulator was fabricated from a 12.5 mm (1/2") diameter PVC pipe and it consisted of three components (sprayer arm, sprayer unit and flow regulator). The rainfall simulator was placed at about 1.0 m on top of the slope model; this height was chosen to preserved the simulated rainfall's terminal velocity and diameter and to ensure that the simulated rainfall successfully drop on the soil surface due to the small nature of the model width. This follows the observation of van Boxel [18] that most rainfall simulators are lower than 2 m height.

Tensiometers (Model 2100F Soil Moisture Probe [19] were used as soil suction measurement instrument in the study. The vacuum gauge of the tensiometers were replaced with a Current Transducer of Model 5301-B1 [20] for automated suction measurement using CR10x model (Campbell Scientific Inc.) data logger. The data from the data logger unit are transferred to computer periodically through serial ports. Prior to the laboratory experiments, the data logger and the tensiometers were tested and calibrated. The schematic diagram of the complete system is shown in Figure 1.

2.2. Soil Sample preparations and experimental work

2.2.1. Soil Sample preparations. The prepared soil samples were compacted in the slope model in layers with thickness of each layer been 100 mm. The required mass per 100 mm thickness was mixed with the residual water content of the soil obtained from Soil Water Characteristics Curve (SWCC) so as to simulate the soil initial condition of the soil prior to the testing. The prepared soil samples were compacted in the model at their maximum dry density. A layer of grade V soil was prepared (about 0.3 m thick) then a transport layer (made from sand or gravel as the case may be) were place above the grade V and finally a grade VI layer was placed. As suggested by [21] a plastic net is placed at each interface to avoid soil particle migration between compacted layers. Figure 2 shows the laboratory slope model during testing.

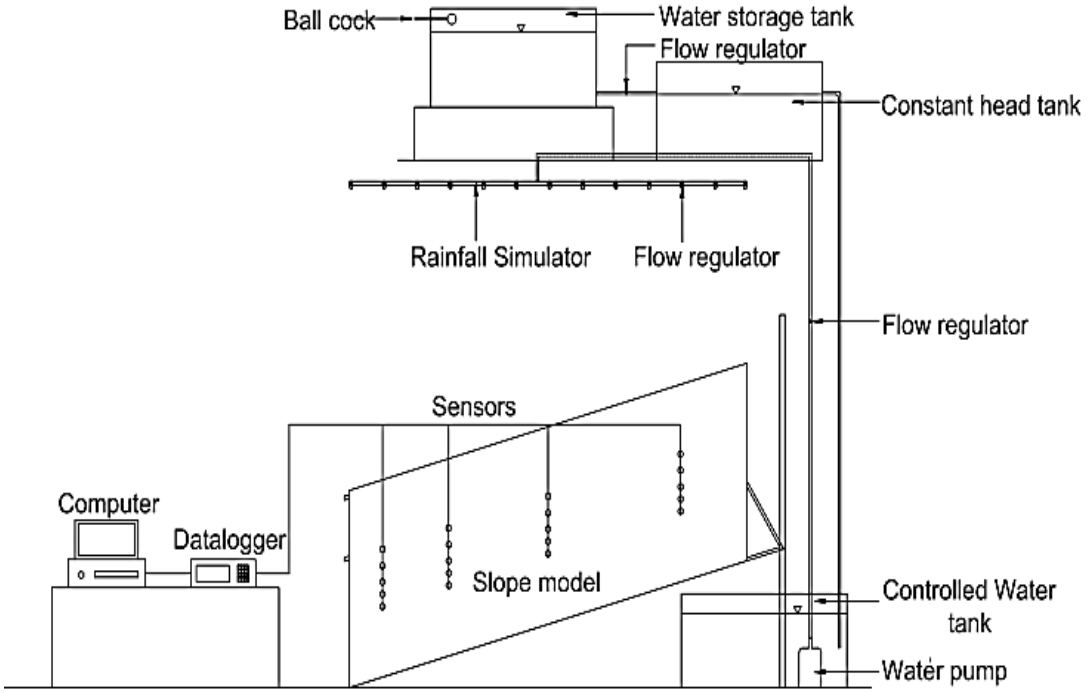

Figure 1. Schematic diagram of the general laboratory modelling setup.

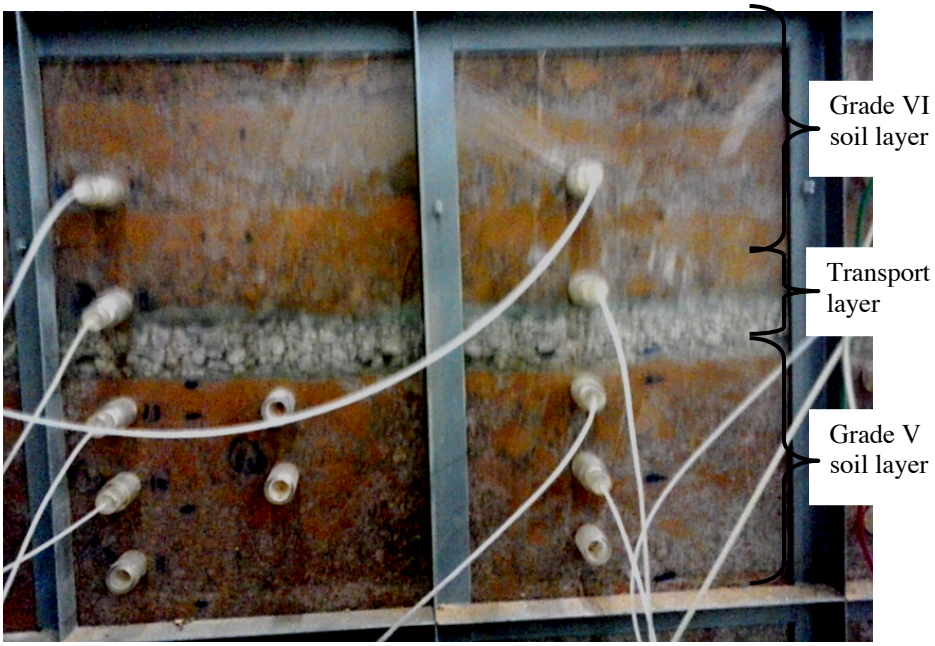

Figure 2. Section of prepared laboratory slope model with soils and transport layer before testing.

*2.2.2 Experimental s*chemes. The experimental program adopted in this study was parted into five (3) schemes. The first scheme was designed to study the natural capillary barrier effect that exists in tropical residual soil mantle due to weathering process. Under this scheme, four extreme rainfall intensities i.e. 1-hour, 2-hour, 24-hour and 7-day were used. However, because the infiltrating water

due to 1-hour rainfall pattern does not reach the interface of the two soil layers, it was subsequently omitted in the remaining experimental schemes. The performance of two transport layers (i.e. Gravel and Sand) were studied in the remaining two schemes.

2.2.3. Rainfall characteristics. Four rainfall intensities were applied to the prepared soil sample compacted in the slope model through a rainfall simulator. These rainfall intensities were determined from an Intensity-Duration-Frequency (IDF) curve of Johor Bahru, Malaysia. The IDF curve for ten-year return period, was developed using an equation 1 recommended by Department of Irrigation and Drainage (DID), Malaysia and Gumbel [22] distribution.

$$ln\,({}_{R}I_{t}) = a + bln(t) + c(ln(t))^{2} + d(ln(t))^{3} \quad (1)$$

Where, ${}_{R}I_{t}$ = average rainfall intensity (mm/hr) for average recurrence interval (ARI) and duration t, R = Average return intervals (years), t = Duration (minutes), a, b, c and d are fitting constants which depends on return period and geographical location.

The developed IDF curve is presented in Figure 3. From Figure 3, it is apparent that the total rainfall amount increases with the increase in time whereas the rainfall intensity decreases with the duration, which is typical rainfall characteristics i.e. for short duration, usually the intensity is high while for long duration, the intensity is usually low. Eventually, four rainfall intensities [1-hour rainfall intensity (1.72×10^{-5} m/s), 2-hour rainfall intensity (1.06×10^{-5} m/s), 24-hour rainfall intensity (1.20×10^{-6} m/s), and 7-day rainfall intensity (3.73×10^{-7} m/s)] were selected from the IDF curve and were simulated in the laboratory for the two-dimensional slope model experiments. These values represent 70% of the total rainfalls obtained from the IDF curve, the remaining 30% was assumed to contribute to surface loss. This assumption was supported by findings from previous studies such as [23-25].

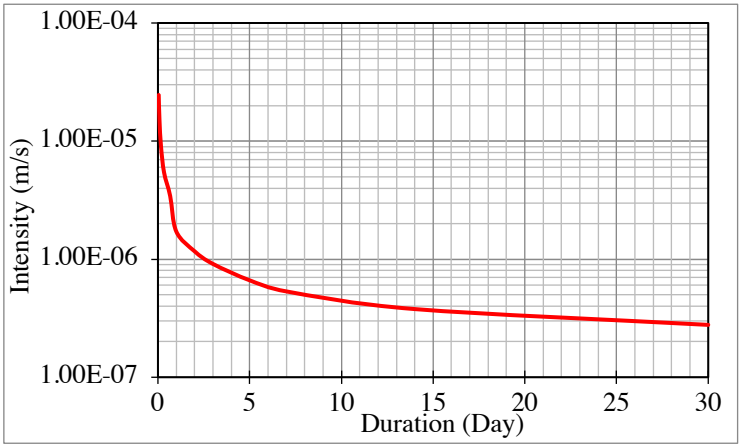

Figure 3. Intensity-Duration-Frequency (IDF) curve of Johor Bahru, Malaysia.

3. Results and Discussion

3.1. Basic soil properties

Figure 4 shows the particle size distribution of grade VI and grade V soils and that of the transport layer materials (i.e. sand and gravel). The grade VI and grade V soils are both classified as sandy silt of very high plasticity (MVS) and silty gravel of high plasticity (MHG), respectively. According to British Standard Classification System. The summary of the basic soil properties used in the study is presented in Table 1.

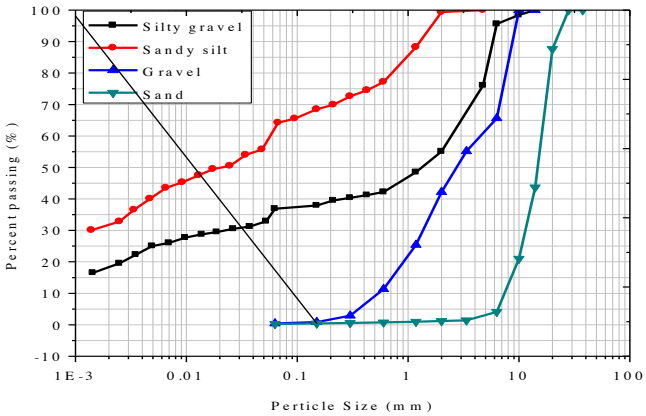

Figure 4. Particle size distribution curves of the soils.

Table 1. Summary of the soil properties used in the study.

Description	**Sandy Silt**	**Silty Gravel**	**Gravel**	Sand
Moisture content, w_n (%)	28	26	-	-
Liquid limit, w_L (%)	78	65	-	-
Plastic Limit, w_P (%)	35	46	-	-
Plasticity Index (*PI*)	23	19	-	-
Soil Classification (*BSCS*)	MVS	MHG	GP	SGPu
Specific gravity, G_s	2.64	2.66	2.7	2.66
Saturated Coefficient of Permeability, k_{sat} (m/s)	$5.89\text{x}10^{-7}$	$1.24\text{x}10^{-6}$	$3.46\text{x}10^{-2}$	$2.88\text{x}10^{-4}$
Maximum dry density, *MDD* (Mg/m^3)	1.42	-	-	-
Optimum moisture content, *OMC* (%)	31	-	-	-

3.2. Breakthrough suction

The breakthrough suction is the minimum negative pore-water pressure at the interface of the two soil layers that signifies breakthrough occurrence. As suggested by [6,7,26], the breakthrough suction was determined as the matric suction where the hydraulic conductivity curves of sandy silt and silty gravel coincided. The breakthrough suction for the soil arrangement is 5 kPa.

3.3. Suction distribution in a two-layered soil system without transport layer

The two-layered residual soil system consists of sandy silt as the upper soil layer and silty gravel as the lower soil layer. The suction distribution with depth and time in the two-layered slope without transport layer due to 2-hour, 24-hour and 7-day rainfall patterns are presented in Figures 5 and 6, respectively.

Figure 5(a) depicts a suction distribution for the 2-hour rainfall pattern This Figure shows a uniform downward progression of infiltrating water at 0.1 m, 0.2 m and 0.3 m depths of the soil profile. The contrast in soil properties between the sandy silt and silty gravel creates a capillary break, which results in accumulation of the infiltrating water above the interface. The accumulated water flows laterally along the interface due to increase in volumetric water content with time. The increase in volumetric water content at the interface of the two soil layers decreases the negative pore-water pressure at 0.3 m depth. However, the negative pore-water pressure at 0.45 m depth remained stable (i.e. 30 kPa) for one hour before it responded to the rainfall infiltration. This finding was supported by that of [23]. At the end of the 2-hour rainfall pattern the negative pore-water pressure at 0.1 m, 0.2 m, 0.3 m and 0.45 m depths are 2 kPa, 3.5 kPa, 5.5 kPa and 24.5 kPa, respectively. This observation shows that the infiltrating water was retained in the sandy silt layer as a result of capillary

barrier effect which impedes downward movement of infiltrating water into the lower silty gravel layer [7].

Figure 6(a) signifies instantaneous increases in the negative pore-water pressure at the beginning of rainfall event, which depicts accumulation of the infiltrating water above the interface of sandy silt and silty gravel soil layers, but it does not penetrate the lower silty gravel layer because of the capillary barrier effect that exists due to the soil arrangement. The negative pore-water pressure at the interface reached the breakthrough suction (5 kPa) at the end of 2-hour rainfall duration. However, the infiltrating water begins to flow downward into the silty gravel layer after 2 hours.

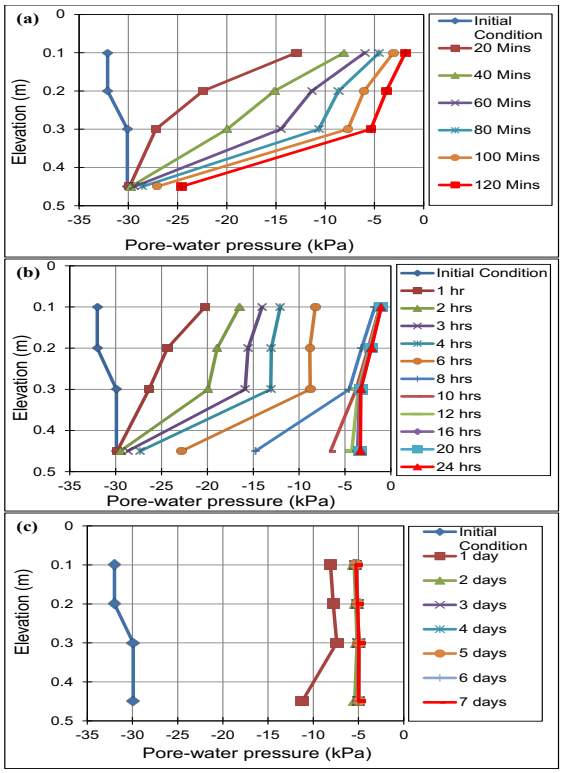

Figure 5. Suction distribution for silty gravel overlain by sandy silt without transport layer due to (a) 2-hour, (b) 24-hour and (c) 7-day rainfall patterns.

The suction distribution due to 24-hour rainfall pattern is presented in Figure 5(b). At the early stage of the rainfall, the variation in the negative pore-water pressure with depth is nearly similar to that of 2-hour rainfall pattern. A uniform downward progression of infiltrating water is observed at 0.1 m, 0.2 m and 0.3 m depths. However, as rainfall continues, more water infiltrates the sandy silt layer and accumulates above the interface. A hydrostatic equilibrium was observed in the sandy silt layer 6 hours after rainfall infiltration and the negative pore-water pressure profile in the sandy silt remained constant throughout the depth (i.e. 8.5 kPa) which implies the sandy silt layer have approached a unit slope (i.e. no change in gradient). The negative pore-water pressure at 0.45 m depth responded to infiltrating water after 2 hours of rainfall infiltration, which indicates the infiltrating water have percolated into the silty gravel layer. A total breakthrough in to the silty gravel layer occurred after 8 hours of rainfall infiltration and the infiltrating water was no longer retained in the sandy silt layer, because the capillary forces present in the sandy silt layer have been demobilized by infiltrating water. The suction distribution in the sandy silt layer remained nearly the same after breakthrough occurrence. Perhaps, after 10 hours of rainfall infiltration, more water infiltrated the whole slope profile and the soils achieved a unit gradient (i.e. equilibrium condition).

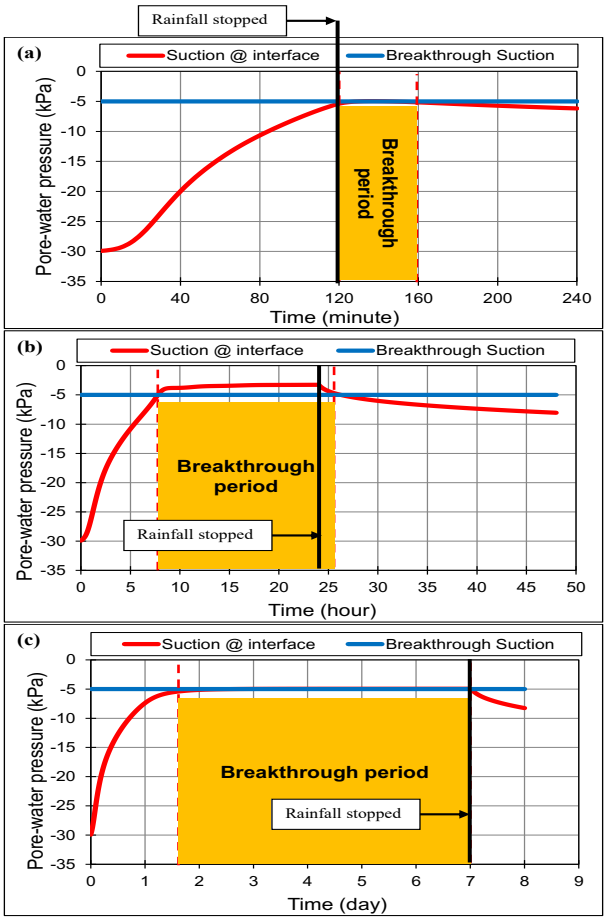

Figure 6. Suction distribution with time along the interface of sandy silt and silty gravel due to (a) 2-hour, (b) 24-hour and (c) 7-day rainfall patterns.

In Figure 6(b), the negative pore-water pressure decreases quickly from the initial soil suction of 32 kPa until it reaches the breakthrough suction after 8 hours of rainfall infiltration. It became constant and uniform after the 9 hours, which indicates water breakthrough occurrence into the silty gravel layer. Unlike in the case of 2-hour rainfall infiltration where the negative pore-water pressure coincided with the breakthrough suction value after breakthrough occurrence; the negative pore-water pressure due to this rainfall pattern decreases beyond the breakthrough suction value. This occurred due to longer time of the rainfall infiltration compared to the 2-hour rainfall pattern.

The suction distribution for 7-day rainfall pattern is shown in Figure 5(c). From this Figure, significant inflow of infiltrating water throughout the two soil layers was observed in the first 1 day of rainfall infiltration. The negative pore-water pressure observed at 0.3 m depth (7.5 kPa) is slightly lower than 8.2 kPa observed at 0.1 m depth. This clearly shows that the infiltrating water have accumulated above the interface of the two soil layers due to contrast in the soil properties which forms a capillary break. The accumulation of water at the interface increases the volumetric water content of the soil, which decreases the negative pore-water pressure. Although there is significant inflow of infiltrating water throughout the soil profile in the first 1 day, the negative pore-water pressure at 0.45 m depth (i.e. 12 kPa) is higher than the negative pore-water pressure at interface (i.e. 7.5 kPa). This indicates more water still infiltrates the silty gravel layer. A total breakthrough has occurred in the second day of rainfall infiltration, and full saturation throughout the soils profile was observed in the second day. This implies occurrence of hydrostatic equilibrium throughout the soil

profile. The breakthrough occurrence, results in uniform negative pore-water pressure (i.e. 5.5 kPa) throughout the soil profile, which also confirmed the total breakthrough occurrence. For the 7-day rainfall pattern as shown in Figure 6(c), the negative pore-water pressure similarly decreases instantaneously until it reaches the breakthrough suction value after 1 day and 14 hours. Beyond this time, it became constant, uniform and approximately equal to the breakthrough suction value until the 7 days elapsed. However, as observed in Figure 5.4, the negative pore-water pressure after the 8th day is approximately equal to 8.3 kPa. This is because after the rainfall was stopped at the 7th day the suction redistribute in the remaining 1 day considered for the analysis.

3.4 Suction distribution in a two-layered soil system with gravel transport layer

The variation of suction distribution with depth and time in the two-layered slope with gravel transport layer due to 2-hour, 24-hour and 7-day rainfall patterns are presented in Figures 7 and 8, respectively.

The suction distribution with depth due to 2-hour rainfall pattern was shown in Figure 7(a). The uniform downward progression of infiltrating water is limited to 0.1 m and 0.2 m depths. The infiltrating water accumulates above the transport layer-sandy silt interface and diverted laterally above the interface and through the transport layer. This is indicated by rapid variation in the negative pore-water pressure at 0.2 m depth due to increase in the volumetric water content. Unlike in the case of two-layered slope without transport layer where the infiltrating water reached the depth of 0.45 m, the infiltrating water for this scheme does not reached this depth. This is because the negative pore-water pressure at 0.45 m depth remained the same as that of initial condition before the test commenced. After 1 hour of rainfall infiltration, there is too much water in the sandy silt soil layer, which results in development of positive pore-water pressure in the sandy silt soil layer. This occurred because the infiltrating water was impeded from percolating the silty gravel layer due to large contrast in particle sizes between the sandy silt and gravel transport layer. For the 2-hour rainfall pattern as shown in Figure 8(a), the negative pore-water pressure was maintained as 30 kPa for 40 minutes of rainfall infiltration. This signifies the infiltrating water was retained in the sandy silt layer within this period and does not reached the interface. However, the infiltrating water accumulates in the transport layer and increases the volumetric water content after 40 minutes of rainfall infiltration. This invariably reduces the negative pore-water pressure to 23 kPa. It was then effectively diverted through the transport layer. This is evident from the values of negative pore-water pressure at the interface, which was maintained as 23 kPa throughout the rainfall duration.

The suction distribution with depth due to 24-hour rainfall pattern is presented in Figure 7(b). There is uniform downward progression of infiltrating water at 0.1 m and 0.2 m depths of the sandy silt layer. The negative pore-water pressure at the transport layer – sandy silt interface is slightly lower than the negative pore-water pressure at 0.1 m depth after 2 hours of rainfall infiltration. This occurred due to the increase in volumetric water content because of continuous rainfall infiltration, which accumulates above the interface. The infiltrating water was effectively diverted above the transport layer – sandy silt interface at the initial stage of the 24-hour rainfall pattern. This was indicated by the decrease in negative pore-water pressure due to increase in volumetric water content at 0.2 m depth. However, the infiltrating water flows laterally through the transport layer after percolating the gravel transport layer. This is evident from the changes in the negative pore-water pressure, from 30 kPa to 29 kPa at 0.3 m depth. The positive pore-water pressure also developed due to this rainfall pattern after 4 hours of rainfall infiltration. A hydrostatic equilibrium condition is reached in the sandy silt layer and the suction profile approached a unit slope (i.e. no change in gradient) after 4 hours of rainfall infiltration. The suction distribution with time due to 24-hour rainfall is presented in Figure 8(b). From this Figure, significant amount of the infiltrating water was effectively diverted above the transport layer – sandy silt interface.

The suction distribution due to 7-day rainfall pattern is presented in Figure 7(c). In a two-layered slope without transport layer, the infiltrating water percolated the whole depth of the soil profiles in the first one day. However, it was effectively diverted due to the influence of transport layer in this

arrangement. A significant inflow of water in to the silty gravel layer was observed after the third day of rainfall infiltration. Similarly, positive pore-water pressure has also developed due to this rainfall pattern between 1 day and 3 days. Within these periods the infiltrating water flows laterally above the transport layer-sandy silt interface and through the transport layer.

A full saturation throughout the soil profile was observed from the fifth day until the end of the rainfall duration and the negative pore-water pressure remained unchanged throughout the soil profiles. This also signifies percolation of the infiltrating water throughout the soil profile. It's worth knowing that even with percolation of water into the silty gravel layer the negative pore-water pressure at interface does not reached the total breakthrough suction of -1.5 kPa when a transport layer is considered. The suction distribution with time due to 7-day rainfall pattern is presented in Figure 8(c). From this Figure, the infiltrating water was diverted laterally above the transport layer – sandy silt interface in the first 1 day of rainfall infiltration. However, it penetrates the gravel transport layer after 1 day and it implies the volumetric water content in the sandy silt layer have increased enough to remove the capillary forces present due to capillary barrier effect.

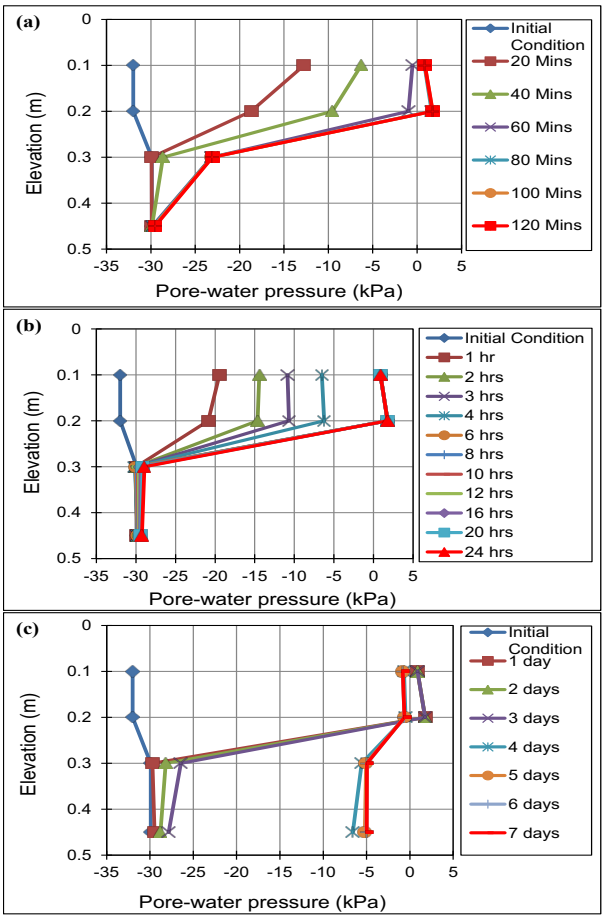

Figure 7. Suction distribution for silty gravel overlain by sandy silt with Gravel transport layer due to (a) 2-hour, (b) 24-hour and (c) 7-day rainfall patterns.

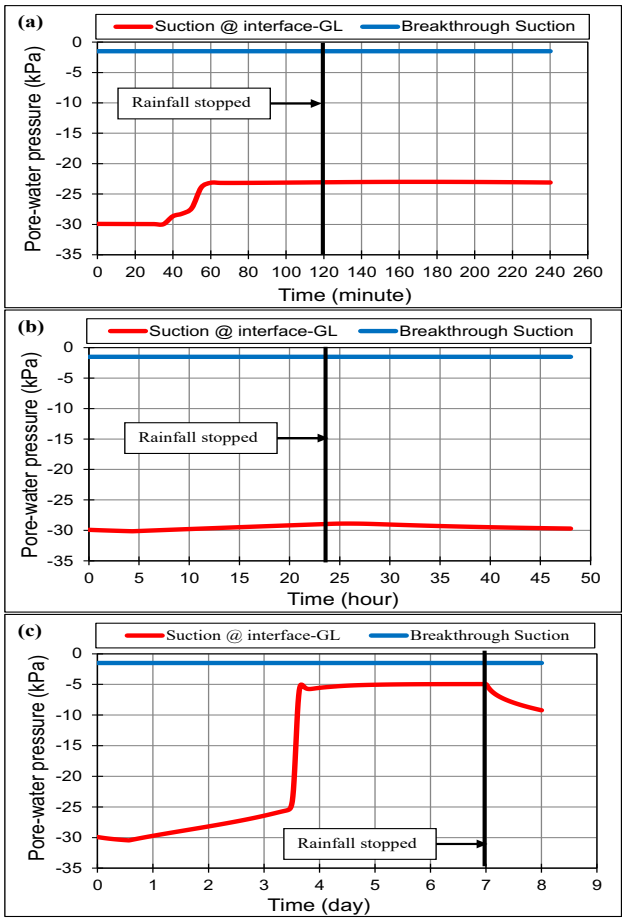

Figure 8. Suction distribution with time along the interface of sandy silt and gravel transport layer due to (a) 2-hour, (b) 24-hour and (c) 7-day rainfall patterns

3.5 Suction distribution in a two-layered soil system with sand transport layer

The variation of suction distribution with depth and time in the two-layered slope with sand transport layer due to 2-hour, 24-hour and 7-day rainfall patterns are presented in Figures 9 and 10, respectively.

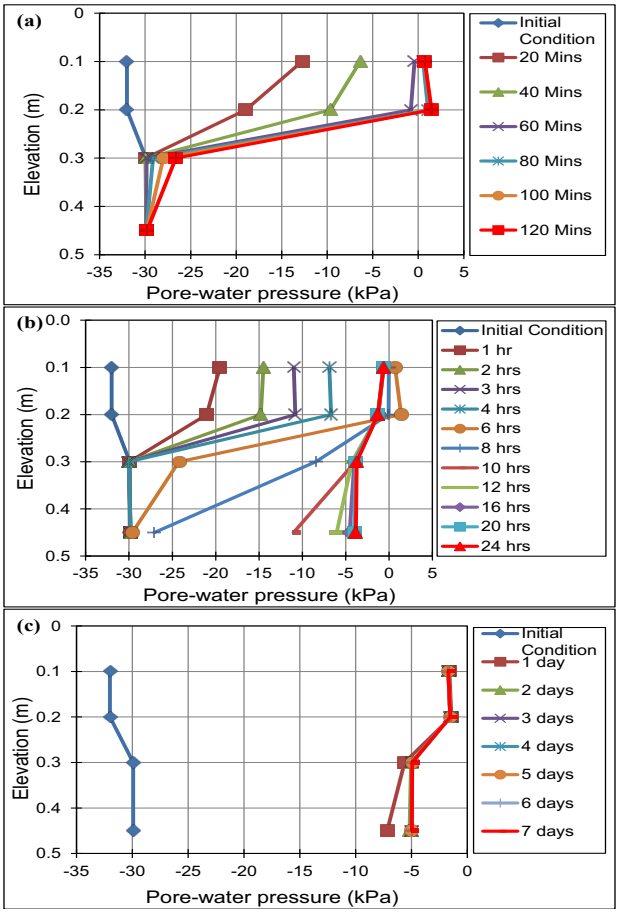

Figure 9. Suction distribution for silty gravel overlain by sandy silt with sand transport layer due to (a) 2-hour, (b) 24-hour and (c) 7-day rainfall patterns.

The suction distribution with depth for 2-hour rainfall is shown in Figure 9(a). This Figure also shows a uniform progression of infiltrating water at 0.1 m and 0.2 m depths (i.e. sandy silt soil layer). However, the infiltrating water was diverted above the transport layer – sandy silt interface due to capillary break developed as a result of disparity in soil properties between the two soil layers. This is evident from rapid decrease in negative pore-water pressure with time (at 0.2 m depth) due to increase in volumetric water content as rainfall infiltration continues. Due to high intensity nature of this rainfall pattern, some of the infiltrating water penetrates the transport layer and was diverted through it. This was noticed from slight decrease of negative-pore water pressure at 0.3 m depth towards the end of the rainfall duration. The negative pore-water pressure at 0.3 m varies from 30 kPa at the beginning of the rainfall event to 26.5 kPa towards the end of the rainfall event. Figure 10(a) shows the suction distribution with time for the 2-hour rainfall pattern. The negative pore-water pressure at the interface was maintained for 1 hour before it responded to the infiltration. This signifies the infiltrating water was diverted laterally through the transport layer after 1 hour of rainfall infiltration. The water diversion through the transport layer causes the silty gravel-transport layer interface to get wetter, and results in decrease of negative pore-water pressure at the interface. Although, the rainfall duration is 2 hours and the rainfall have stopped after 2 hours, the negative pore-water pressure at the interface continuous to decrease because the infiltrating water retained by the sandy silt layer is been released until this layer has attained an equilibrium condition.

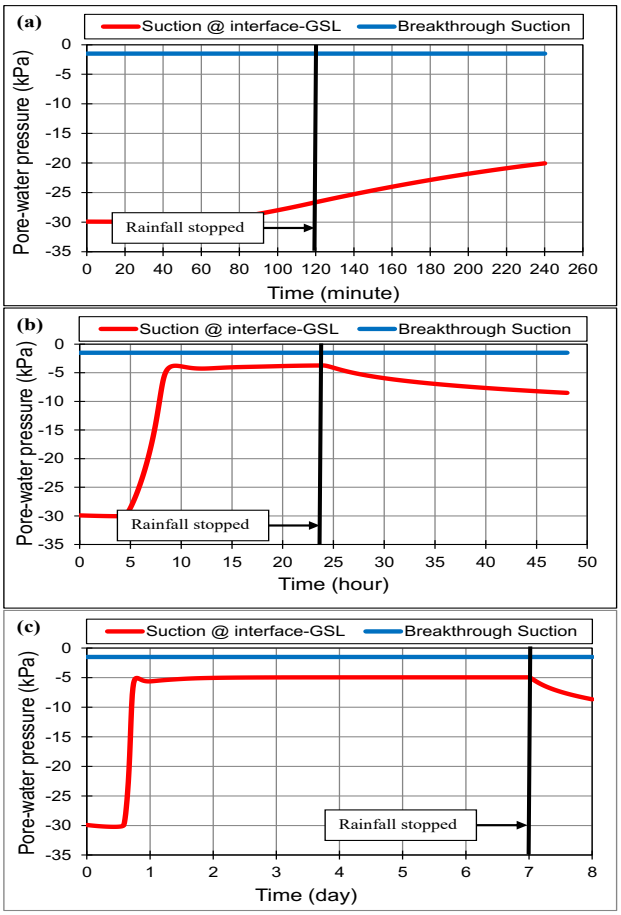

Figure 10. Suction distribution with time along the interface of sandy silt and sand transport layer due to (a) 2-hour, (b) 24-hour and (c) 7-day rainfall patterns.

The suction distribution due to 24-hours rainfall pattern is presented in Figure 9(b). This Figure shows a uniform downward progression of water at 0.1 m and 0.2 m depths of the sandy silt layer due to decrease in negative pore-water pressure because of increase in volumetric water content. The infiltrating water was diverted above the transport layer-sandy silt interface. However, after 5 hours of rainfall infiltration, there is significant amount of infiltrating water in the sandy silt soil layer, which results in development of positive pore-water pressure in the sandy silt layer. Perhaps, after 6 hours of rainfall infiltration, the infiltrating water percolates the gravelly sand transport layer and flow laterally. This was noticed from the decreased in negative pore-water pressure from 30 kPa to 24.5 kPa at 0.3 m depth. The infiltrating water percolates the lower silty gravel layer after 8 hours of rainfall infiltration. This is evident from how negative pore-water pressure decreases from 30 kPa to 26.5 kPa at 0.45 m depth. The percolation of the infiltrating water into the silty gravel layer also results in regaining of negative pore-water pressure in the sandy silt soil layer. The suction distribution with depths remained constant after 15 hours of rainfall infiltration. This indicates full saturation throughout the depth of soil layers was attained and the negative pore-water pressure at the interface decreases to 4 kPa which is still below the breakthrough suction value. The suction distribution with time for the 24-hour rainfall pattern is presented in Figure 10(b). The Figure shows that the infiltrating water was diverted above the transport layer-sandy silt interface for 5 hours. However, the infiltrating water was further diverted through the transport layer after 5 hours of rainfall infiltration. Perhaps, continuous rainfall infiltration increases the volumetric water content at the silty gravel-transport layer interface, which decreases the negative pore-water pressure at that

interface. This causes the diverted water through the transport layer to percolates the silty gravel layer, which results in full saturation of the soil profile. The suction at the interface remained constant until the end of the rainfall duration and it increases about 1 hour after the rainfall has stopped until the end of analysis period (i.e. 48 hours).

The suction distribution with depth for 7-day rainfall pattern is presented in Figure 9(c). From this Figure, the infiltrating water was diverted laterally above the transport layer-sandy silt interface and through the transport layer in the first one day of rainfall infiltration. However, diversion of water through the transport layer due to continuous rainfall infiltration, increases volumetric water content at silty gravel-transport layer interface which in turn decreases the negative pore-water pressure at the interface to 6.5 kPa. Similarly, a full saturation throughout the soil profile was observed in the second day of rainfall infiltration and the negative pore-water pressure remained constant with time throughout the soil profile. The suction distribution with time for the 7-day rainfall pattern is presented in Figure 10(c). Similar trend like that of 24-hour rainfall pattern was observed in 7-day suction distribution with time. The infiltrating water was diverted above the transport layer-sandy silt interface and through the transport layer for about 12 hours. However, due to increase in the volumetric water content as a result of continuous rainfall infiltration the infiltrating water percolates the silty gravel layer after 12 hours of rainfall infiltration. Perhaps, the negative pore-water pressure at the interface decreases to 5 kPa instantly. The negative pore-water pressure at the interface remained constant until the end of rainfall duration (i.e. 7 days). Similarly, it continuous to redistribute immediately after the rainfall has stopped.

The findings of this study are in accordance with that of previous researchers such as [7] who found that a total breakthrough suction value is achieved after prolonged rainfall infiltration. This phenomenon has been discussed and explained by numerous researches such as [6, 11, 26, 27, 28, 29] among others.

4. Conclusions

A two-dimensional laboratory model was constructed to investigate the effect of transport layer in the diversion capacity of natural capillary barrier system. The following conclusions can be drawn from the results of the laboratory studies:

i. The natural arrangement of grade VI (sandy silt) and grade V (silty gravel) produces a natural capillary barrier effect that restrain downward movement of infiltrating water into the deeper depth and facilitate lateral flow of the water along the interface with minimal diversion length.
ii. The introduction of transport layer at the interface of the sandy silt and silty gravel modifies the diversion capacity and restrained excessive percolation of the infiltrating water into the deeper depth.
iii. Gravel material modified the diversion length and hence more effective compared to sand due to larger particle contrast between the two materials.

Acknowledgement

The first author acknowledges the Management of Bayero University, Kano and TET Fund Nigeria for approving and sponsoring the conference attendance.

References

[1] S. Zhanga X Zhanga X Peia S Wangb R Huanga Q Xua and Z Wanga 2019 *Eng. Geo.* **258** 14
[2] L L Zhang L M Zhang and W H Tang *Géotechnique*. **55**(2) 6
[3] H Rahardjo K K Aung E C Leong and R B Rezaur *Eng. Geo.* **73** 13
[4] H Rahardjo X W Li D G Toll and E C Leong *Geotech. & Geol. Eng.* **19** 29
[5] C E Morris and J C Stormont D 1997 *J. Env. Eng.* **123**(1) 8
[6] J H Li L Du R Chen and L M Zhang 2013 *Comp. & Geotech.* **48** 12
[7] B. Ross 1990 *Wat. Res. Res.* **26**(10) 5

[8] J C Stormont 1996 *Geotech. & Geol. Eng*. **14**(4) 25
[9] H Yang H Rahardjo E C Leong D G Fredlund 2004 *Can. Geotech. J.* **41**(4) 15
[10] C M Oldenburg K Pruess 1993 *Wat. Res. Res.* **29**(4) 11
[11] M T Walter J S Kim T S Steenhuis J Y Parlange A Heilig R D Braddock J S Selker and J Boll 2000 *Wat. Res. Res.* **36**(4) 9
[12] N Lu J W Godt 2013 *Hillslope Hydrology and Stability* (Cambridge University Press)
[13] N Lu and W J Likos 2004 *Unsaturated Soil Mechanics* (Hoboken, New Jersey: John Wiley & Son, Inc.).
[14] C E Morris and J C Stormont 1999 *J. Geotech. & Geoenv. Eng.* **125**(12) 9
[15] T S Steenhuis J Parlange and K J S Kung 1991 *Wat. Res. Res.* **27**(8) 2
[16] J Smesrud and J Selker 2001 *J. Geotech. & Geoenv. Eng.* **127**(10) 4
[17] L T Zhan W Jiao L Kong and Y M Chen 2014 *Geo-Congress* 10
[18] J H van Boxel 1997 *Workshop on Wind and water erosion, Ghent, Belgium*
[19] Soil Moisture Equipment Corp. *Operating Instructions for 2100F Soil Moisture Probe*. (Soil Moisture Equipment Corp. Santa Barbara USA (2009b).
[20] Soil Moisture Equipment Corp. *Operating Instructions for 5301 Current transducer.* Soil Moisture Equipment Corp. Santa Barbara, USA (2012).
[21] H Rahardjo V A Santoso E C Leong Y S Ng and C J Hua P 2012 *J. Geotech. & Geoen. Eng.* **138**(4) 10
[22] E J Gumbel 1958 *Statistics of Extremes* (Columbia University Press. New York)
[23] A Kassim G Nurly L M Lee and H Rahardjo 2012 *Eng. Geo.* **131–132**, 13(2012)
[24] L M Lee G Nurly and H Rahardjo 2009 *Eng. Geo.* **108**(3–4) 16
[25] G Nurly and L M Lee 2008 *Georisk* **2**(2) 14
[26] S-É Parent and A Cabral 2006 *Geotech. & Geol. Eng.* **24**(3) 22
[27] T Miyazaki 1988 *J. Hydr.* **102**(1) 14
[28] M Kampf and T Holfelder H 1998 *Proceedings of the 3rd International Conference on Hydro-Science and Engineering* Berlin, Germany
[29] J C Stormont and C E Anderson 1999 *J. Geotech. & Geoenv. Eng.* **125**(8) 8